

# A Role for HAPLN1 During Phenotypic Modulation of Human Lung Fibroblasts In Vitro

Stephen P. Evanko, Michel D. Gooden, Inkyung Kang, Christina K. Chan, Robert B. Vernon, and Thomas N. Wight\*

Matrix Biology Program, Benaroya Research Institute at Virginia Mason, Seattle, WA, USA (SPE, MDG, IK, CKC, RBV, TNW)

## Summary

Hyaluronan and proteoglycan link protein 1 (HAPLN1) stabilizes interactions between two important extracellular matrix (ECM) macromolecules, versican and hyaluronan, which facilitate proliferation of fibroblasts and their conversion to myofibroblasts. However, the role of HAPLN1 in these events has not been studied. Using immunocytochemistry, cellular and ECM locations of HAPLN1 were evaluated in cultured human lung fibroblasts during proliferation and conversion to myofibroblasts. HAPLN1 localized to pericellular matrices, associating with both versican and hyaluronan in the ECM and on the cell surface. Nuclear and total HAPLN1 immunostaining increased after myofibroblast induction. Confocal microscopy showed HAPLN1 predominant in the ECM under cells while versican predominated above cells. Versican and HAPLN1 were also juxtaposed in columnar inclusions in the cytoplasm and nucleus. Nuclear HAPLN1 staining in interphase cells redistributed to the cytosol during mitosis. In the absence of TGF- $\beta$ 1, addition of exogenous bovine HAPLN1 (together with aggrecan G1) facilitated myofibroblast formation, as seen by significant upregulation of  $\alpha$ -smooth muscle actin (SMA) staining, while adding full-length bovine versican had no effect. Increased compaction of hyaluronan-rich ECM suggests that HAPLN1 plus G1 addition affects hyaluronan networks and myofibroblast formation. These observations demonstrate changes in both extracellular and intracellular localization of HAPLN1 during fibroblast proliferation and myofibroblast conversion suggesting a possible role in fibrotic remodeling. (J Histochem Cytochem 68: 797–811, 2020)

## Keywords

extracellular matrix, fibroblasts, glycosaminoglycans, hyaluronan, immunohistochemistry, link protein, mitosis, myofibroblasts, nucleus, proteoglycans, versican

## Introduction

Hyaluronan and proteoglycan link protein 1 (HAPLN1), is a hyaluronan-binding protein (hyaladherin) that was originally characterized in cartilage proteoglycan preparations, and was shown to stabilize the interaction of aggrecan and hyaluronan in large multi-molecular aggregates that form the chondrocyte pericellular matrix.<sup>1,2</sup> HAPLN1 also stabilizes the interaction of other aggregating chondroitin sulfate (CS) proteoglycans, such as versican and neurocan with hyaluronan.<sup>3–5</sup> HAPLN1 shares about 95% sequence homology with aggrecan and versican G1 domains. These molecules exhibit tight

binding to hyaluronan with  $K_d$  in the range of  $10^{-8}$  M and occupy about 6–7 disaccharides,<sup>6</sup> but, unlike the proteoglycan monomers, their binding to hyaluronan is not decreased at pH 5.<sup>7</sup> Link protein deletion in transgenic animals resulted in chondrodysplasia and perinatal lethality, while overexpression had no

Received for publication July 31, 2020; accepted September 23, 2020.

\*Member of The Histochemical Society at the time of publication.

### Corresponding Author:

Thomas N. Wight, Matrix Biology Program, Benaroya Research Institute at Virginia Mason, 1201 Ninth Avenue, Seattle, WA 98101, USA.  
E-mail: [twight@benaroyaresearch.org](mailto:twight@benaroyaresearch.org)

discernable phenotype.<sup>8</sup> HAPLN1 also stabilizes the perineuronal nets (PNNs) in neurons as evidenced by HAPLN1 deletion in the brain leading to attenuated PNNs.<sup>9</sup> HAPLN1 was recently shown to impact collagen organization in dermal fibroblasts and immune cell infiltration,<sup>10</sup> promoting tumor metastasis.<sup>11</sup> Such observations suggest a role for HAPLN1 in events leading to fibrosis. Modulation of myofibroblast formation is a potential target for treating lung fibrosis. Hyaluronan and its binding partners have been shown to be important and play complex roles in the fibroblast/myofibroblast transition.<sup>12–14</sup> Lung fibrosis is primarily regulated by TGF- $\beta$ 1, which is known to increase hyaluronan, versican, and other extracellular matrix (ECM) molecules such as collagen, fibronectin, and tenascin, in addition to the characteristic increased expression of  $\alpha$ -smooth muscle actin ( $\alpha$ -SMA),<sup>15–18</sup> but the role of HAPLN1 in lung fibroblast-to-myofibroblast conversion has not been explored.

Our earlier studies have shown also that hyaluronan- and versican-dependent pericellular matrix formation was required for proliferation and migration of smooth muscle cells (SMCs)<sup>19</sup> and that intracellular hyaluronan was associated with proliferation of fibroblasts and SMCs.<sup>20,21</sup> In addition, stimulation of proliferation with platelet-derived growth factor (PDGF) also increased production of both versican and HAPLN1, and the amount of link-stabilized aggregates in the ECM of SMCs,<sup>22</sup> but it was unclear whether HAPLN1 interacted with both of these two components not only outside of cells, but also inside cells as well. The unusual intracellular localization of hyaluronan during cellular proliferation led us to wonder whether other hyaladherins such as HAPLN1 are present inside cells and associate with the proliferative cell phenotype.

This study used immunocytochemistry to probe the location of HAPLN1 in cultures of lung fibroblasts and TGF- $\beta$ 1-induced myofibroblasts. HAPLN1 localized with hyaluronan and versican in the pericellular matrix and was enriched underneath cells in adhesive structures. HAPLN1 was also enriched with versican in the nuclei of myofibroblasts and interphase cells, and transitioned to the cytosol during mitosis. We also found that a purified hyaluronan binding preparation containing HAPLN1 and aggrecan G1, dramatically altered ECM compaction, and potently stimulates myofibroblast formation, while full-length versican had no effect. Collectively, these observations suggest that both intracellular and ECM-associated HAPLN1 and its binding partners participate in fibroblast proliferation and transformation into myofibroblasts.

## Methods

### Antibodies and Reagents

Monoclonal mouse Anti-HAPLN1 (Crt11), clone 8-A-4 (MilliporeSigma, Burlington, MA; cat # MABT85, lot # 3071955) was used at 1:200. Monoclonal antibody 8A5, also specific for human link protein, was the generous gift of Dr. Duncan Hiscock (University of Wales, Cardiff) and was used at 1/500. Monoclonal mouse anti-human SMA, clone 1A4, (Dako, Carpinteria, CA; Cat # M0851, lot # 20011631) was used at 1:200. Polyclonal rabbit anti-Vc, anti-human versican, a kind gift from Dr. Richard LeBaron<sup>23</sup> was used at 1:2000. Rabbit anti-alpha tubulin antibody was purchased from Abcam (Cambridge, UK; # ab4074) and mouse anti-TGF- $\beta$ 1,2,3 pan-specific antibody was purchased from R&D Systems (Minneapolis, MN; MAB1835). Non-biotinylated hyaluronan binding protein (HABP) and biotinylated HABP (b-HABP) were prepared from bovine nasal septum cartilage by a hyaluronan affinity column as previously described.<sup>24</sup>

Assessment of the HABP by SDS PAGE revealed a single prominent protein band at ~45 kDa and small amounts of CS-containing fragments of aggrecan (data not shown) and the preparation was endotoxin-free (<1.0 EU/ $\mu$ g) as assessed using a ToxinSensor™ LAL Endotoxin Assay Kit (GenScript Corp., Piscataway, NJ). Versican was purified from bovine aorta by a combination of 4 M guanidinium HCL extraction, ion exchange, and size exclusion chromatography, as described previously.<sup>25,26</sup> The versican preparation was free of contaminants as assessed by SDS-PAGE and Coomassie blue and Alcian blue staining, and was also endotoxin-free (<1.0 EU/ $\mu$ g) as assessed using the ToxinSensor™ LAL Endotoxin Assay Kit. The versican specifically bound to b-HABP on ligand blots and to versican-specific antibodies on western blots and comprised the V0 and V1 isoforms (data not shown).

### Cell Culture

Adult normal human lung fibroblasts (HLFs) were obtained from Lonza Biosciences (Bend, OR). A second isolate of HLFs was a generous gift from Professor Ganesh Raghu, Division of Pulmonary and Critical Care Medicine, University of Washington, Seattle. The cells were isolated as described previously in accordance with approval from the institution's human subjects review committee.<sup>27</sup> The HLFs were maintained in Dulbecco's Modified Eagle Medium (DMEM) high-glucose medium supplemented with 10% fetal bovine serum (FBS; HyClone, Logan, UT), 1 mM sodium pyruvate, 0.1 mM non-essential amino acids, 0.43 mg/ml GlutMAX-1, and penicillin-streptomycin

(penicillin G sodium, 100 U/ml, and streptomycin sulfate, 0.10 mg/ml; Invitrogen Life Technologies, Carlsbad, CA) at 37°C in 5% CO<sub>2</sub>. Cells were passaged with trypsin-EDTA (0.05% trypsin and 0.53 mM tetrasodium EDTA) and were used for experiments between passages 8 and 15.

### *Myofibroblast Induction and HABP and Versican Treatment*

Cells were seeded on 22 mm glass coverslips (Corning) at  $3.5 \times 10^5$ /well in 6-well plates in 10% FBS in DMEM. After 24 hr, cells were growth arrested in 0.1% FBS/DMEM for 48 hr, at which point the cells were about 80%–90% confluent. Cells were stimulated with TGF- $\beta$ 1 (10 ng/ml, R&D Systems) for 24 hr. In other experiments, HLF were plated more sparsely at  $1.5 \times 10^5$ /well and a non-biotinylated preparation of HABP containing HAPLN1 or purified full-length bovine versican was added to cells at 10  $\mu$ g/ml, either 1 hr after plating in DMEM containing 10% FBS or after 4 days of growth in 10% FBS. Cells were processed for immunocytochemistry after 4 days.

### *Immunocytochemistry*

Cells on coverslips were fixed for 10 min at 22°C in 10% formalin. Where appropriate ( $\alpha$ -SMA, HAPLN1 staining), cells were also permeabilized in 0.5% Triton X-100 in PBS for 10 min. Following rinsing in PBS, cells were stained for hyaluronan using b-HABP (4  $\mu$ g/ml) or appropriate primary antibody followed by rinsing and streptavidin AF-388 or AF-546 anti-mouse and AF-388 anti-rabbit antibodies (all from Molecular Probes, Eugene, OR, now part of ThermoFisher) (1:500) in PBS containing 1% bovine serum albumin as previously described.<sup>20</sup> For HAPLN1 and hyaluronan co-staining, cells were first incubated with anti-HAPLN1 antibody followed by the b-HABP. Nuclei were stained during mounting with 4',6-diamidino-2-phenylindole (DAPI) at 1  $\mu$ g/ml in Fluorogel mounting medium (Electron Microscopy Sciences, Hatfield, PA). As controls, cells were incubated with normal IgG or predigested with hyaluronan-specific *Streptomyces* hyaluronidase, which abolished staining with the b-HABP.

### *Image Acquisition and Analysis*

Cells were examined using a Leica DMIRB microscope under epifluorescence optics using a 63  $\times$  0.70 numerical aperture objective, and images were acquired using a Spot cooled-charge-coupled device (CCD) camera and imaging program.

Digital images of immunofluorescence (IF)-labeled specimens were also obtained with a Leica TCS-SP5 II confocal microscope (Leica Microsystems, Wetzlar, Germany). A computer module containing Leica Application Suite, Advanced Fluorescence v. 3.3.0.10134.1 imaging software was used to render images in 3-dimensions.

$\alpha$ -SMA staining was quantitated in NIH Image J using thresholded fluorescent images at 20x magnification. In the same field, DAPI-stained nuclei were counted, and staining expressed as  $\alpha$ -SMA-positive pixels per cell ( $n$  equals at least 10 fields per condition, approximately 100–200 cells per field). Nuclear HAPLN1 staining was quantitated using Image J by outlining individual nuclei as a region of interest and expressing pixel density per nucleus ( $n=100$  cells per condition). The density of stained pixels using b-HABP was used as a measure of hyaluronan in the ECM and was assessed using Image J in untreated cells, cells treated with unlabeled HABP, or with full-length bovine versican. Regions of interest were defined specifically and only in the immediate pericellular matrix in thresholded images, and hyaluronan staining intensity was expressed as pixels per area ( $n=100$  cells per condition). Data are representative of at least three individual experiments.

### *Statistical Analysis*

Data were analyzed by one-way ANOVA with a Tukey's multiple comparison test using GraphPad Prism version 7.00 for Windows, GraphPad Software, San Diego, CA, [www.graphpad.com](http://www.graphpad.com).  $p$  values less than 0.05 were considered statistically significant.

## **Results**

### *HAPLN1 Localization*

HAPLN1 was detected in the pericellular matrix and in cytoplasmic and nuclear locations of the HLFs (Fig. 1A and B). Weak to no staining was seen with control mouse IgG (Fig. 1C). Strong staining for HAPLN1 was seen in concentrated deposits located near a nucleus or under lamellipodia. Interestingly, with formalin fixation alone (no distinct permeabilization step) there was a greater proportion of positively stained nuclei in cells arrested in low serum, compared to cells growing in high serum, where most of the staining appeared to be in the pericellular matrix. A nearly identical nuclear and cytoplasmic staining pattern was seen with another monoclonal antibody to HAPLN1, 8A5, further supporting that the staining is specific (data not shown). Quantitation of the

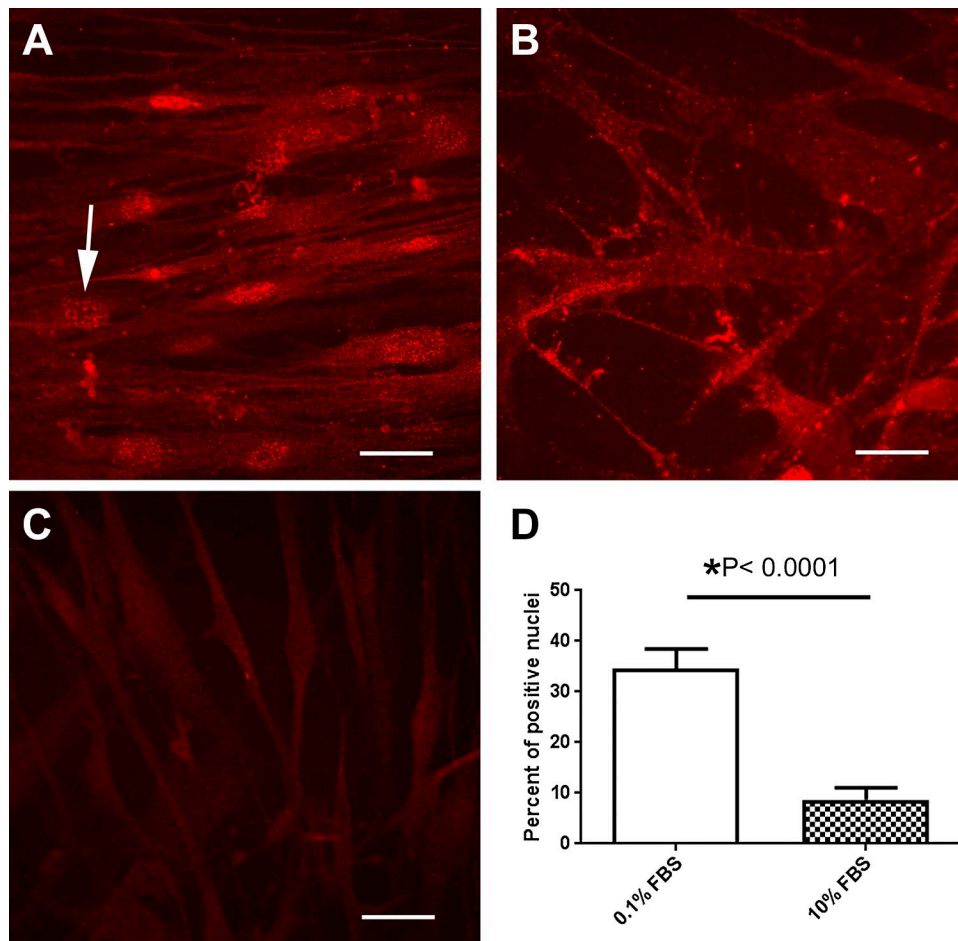


**Figure 1.** HAPLN1 staining (red) in HLFs under (A) quiescent low serum conditions (0.1% FBS) or (B) growing in 10% FBS. The cells were not specifically permeabilized. (C), percentage of positively-stained nuclei in each condition.  $N=10$  fields per condition. Bar equals 25  $\mu\text{m}$ . Abbreviations: FBS, fetal bovine serum; HAPLN1, hyaluronan and proteoglycan link protein 1.

proportion of positive nuclei showed that 35% to 40% of the nuclei in quiescent cells were positive for HAPLN1, whereas less fewer than 10% were positive in actively cycling cells (Fig. 1D). These results suggest that changes in HAPLN1 location are associated with cell proliferation.

HLFs induced to become myofibroblasts by TGF- $\beta$ 1 treatment had slightly higher total HAPLN1 staining ( $p < 0.05$ ) compared to controls in non-permeabilized samples (Fig. 2A to C). When cells were permeabilized before staining, essentially all nuclei were positive in both conditions, except for mitotic cells, and there was significantly increased nuclear staining intensity in TGF- $\beta$ 1-induced myofibroblast nuclei compared to controls ( $p < 0.001$ ) (Fig. 2D to F). This suggests that myofibroblast formation is accompanied by increased amounts of HAPLN1 and its association with nuclei.

In addition to the nuclear staining, co-staining revealed a close association between HAPLN1 and hyaluronan (using b-HABP) in the pericellular matrix around cells in both low- and high-serum conditions (Fig. 3A and B). Staining required sequential incubation, first with the HAPLN1 antibody, then with the b-HABP, so the HAPLN1 in the HABP preparation was not recognized by the monoclonal antibody. Under these conditions, there were very few long coalesced cables of hyaluronan. As seen with digital magnification, the signal for HAPLN1 in the ECM was generally present in two sizes: larger globular deposits  $\sim 45$  nm in diameter (Fig. 3C and D, arrowheads) and also smaller puncta  $\sim 30$  nm, closely aligned along individual strands of hyaluronan (Fig. 3D). These observations are similar to those reported for recombinant versican G1.<sup>28</sup> The larger diameter globules suggest that some aggregation of

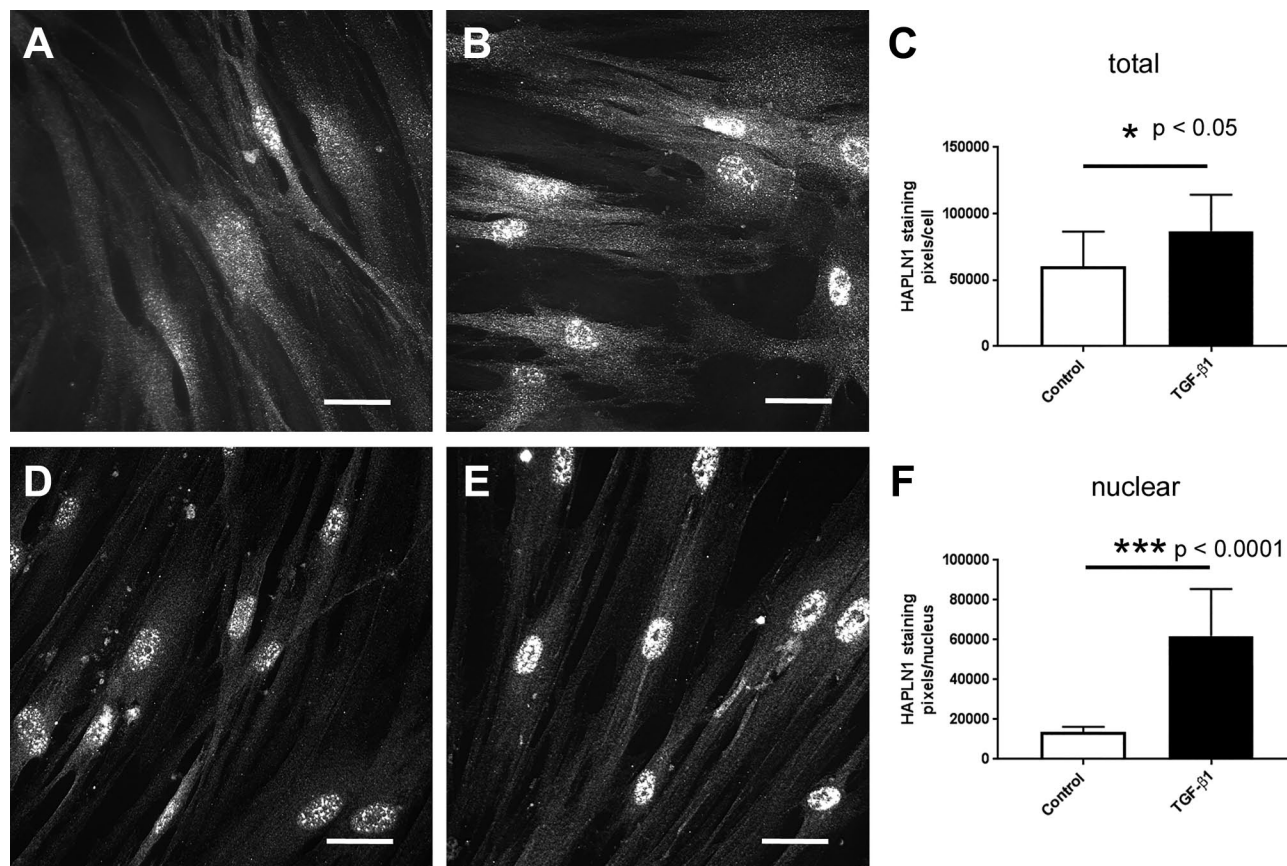


**Figure 2.** (A and B) Non-permeabilized cells, (C), total HAPLN1 staining intensity expressed as pixels per cell.  $N=10$  fields per condition. In (D and E), HLFs were permeabilized before staining. F, nuclear staining intensity expressed as pixels per nucleus.  $N=100$  nuclei per condition. HAPLN1 staining in quiescent control cells (A and D) and TGF- $\beta$ 1-induced myofibroblasts (B and E). Bar equals 25  $\mu$ m. Abbreviation: HAPLN1, hyaluronan and proteoglycan link protein 1; TGF- $\beta$ 1, tumor growth factor  $\beta$ 1.

HAPLN1 or binding to globular forms of hyaluronan may occur. There was a consistent spacing  $\sim 120$  nm between the smallest HAPLN1 signals along the hyaluronan strands, also consistent with the previous report.<sup>28</sup> There is clearly ample space between existing HAPLN1 molecules along the hyaluronan strands to allow the HABP access. In addition to nuclear staining, there was also cytoplasmic staining for HAPLN1, usually in the perinuclear region and also on broad lamellipodia (Fig. 3C, arrow). Thus, HAPLN1 resides in the ECM, within the cytoplasm, and inside the nucleus.

Mitotic cells stained intensely for HAPLN1 in a fashion similar to that previously reported for intracellular hyaluronan.<sup>19</sup> Fig. 4 shows co-staining for HAPLN1 and tubulin in cells growing in medium containing 10% FBS. HAPLN1 was present in the nucleus, which, as noted above, was most pronounced in interphase cells with clearly defined nucleoli (Fig. 4A). During prophase and nuclear membrane breakdown, the nuclear signal diminished and shifted into the

cytoplasm (Fig. 4B and C) and surrounded the chromosomes at metaphase and anaphase (Fig. 4D and E). After telophase, HAPLN1 deposits were observed around the nucleus again (Fig. 4F).

HAPLN1 and versican colocalized with alternating red and green signals, closely juxtaposed along putative individual hyaluronan strands in the pericellular matrix and at the cell surface (Fig. 5). There was also pronounced colocalization of link protein and versican in deposits at membrane adhesive sites, often located near the nucleus of a cell. In many cases, these deposits were oval shaped like the nucleus, and gave the impression that the cell and nucleus had moved, leaving the deposit behind (see also Fig. 8, below). This is suggestive for a role in stabilizing nuclear-ECM connections. In the pericellular matrix, there was a greater abundance of signal for versican compared to HAPLN1, suggesting that not every molecule of versican is associated with HAPLN1.

Confocal microscopy and 3D reconstructions of stacked images with digital processing confirmed

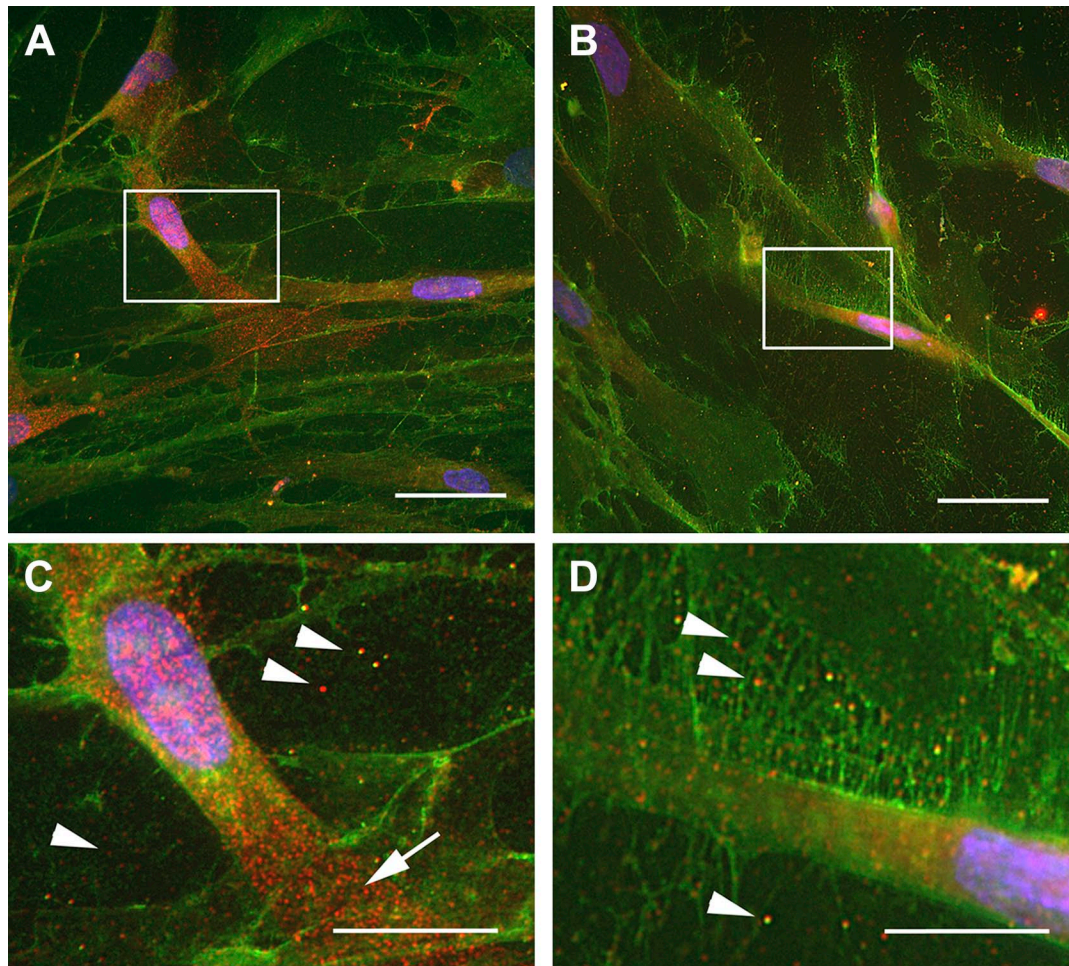


**Figure 3.** HAPLN1 (red) and hyaluronan (green) in HLFs in (A, C), 0.1% FBS or B, D in 10% FBS. HAPLN1 partially localizes to hyaluronan in the pericellular matrix. Boxed areas in (A and B) are enlarged in (C and D). Arrowheads indicate globular deposits of HAPLN1 on hyaluronan in the pericellular matrix. Arrow in C points to HAPLN1 in a broad lamellipodium. Nuclei were stained with DAPI. Bar equals 25  $\mu\text{m}$ . Abbreviations: DAPI, 4',6-diamidino-2-phenylindole; FBS, fetal bovine serum; HAPLN1, hyaluronan and proteoglycan link protein 1; HLF, human lung fibroblasts.

that both versican and HAPLN1 are present in the pericellular matrix, cytoplasm, and within the nucleus (Fig. 6). In an *en face* optical slice, midway through the nucleus (Fig. 6A), signal for both HAPLN1 and versican can be seen in the plane of the nucleus and in cytoplasmic vesicles. In a section in the transverse plane (Fig. 6B and C), HAPLN1 and versican were closely juxtaposed in columnar vesicles in the perinuclear cytoplasm, with some vesicles appearing to extend through the entire thickness of the cell. Fig. 6D shows a maximum projection image of the lateral view to include pericellular matrix from the entire stack of images, but with the cell removed. This revealed that there was a greater abundance of versican in the ECM above the cells relative to HAPLN1, and a higher proportion of HAPLN1 underneath the cells.

Confocal microscopy of mitotic cells in late telophase is shown in Fig. 7, and indicated that versican and HAPLN1 were both abundant in cytoplasmic vesicles, and were present within the connecting mid-body in the area of the cleavage furrow during telophase (Fig. 7).

#### HAPLN1—Cytoskeleton Relationship

We previously reported that hyaluronan and CD44 played an adhesive role, primarily in association with the cortical actin network between stress fibers in fibroblasts and myofibroblasts.<sup>18</sup> In the present study, the relationship of HAPLN1 to the actin cytoskeleton was examined using phalloidin and revealed no or only occasional colocalization with f-actin stress fibers (Fig. 8A). However, remnants of f-actin often were seen

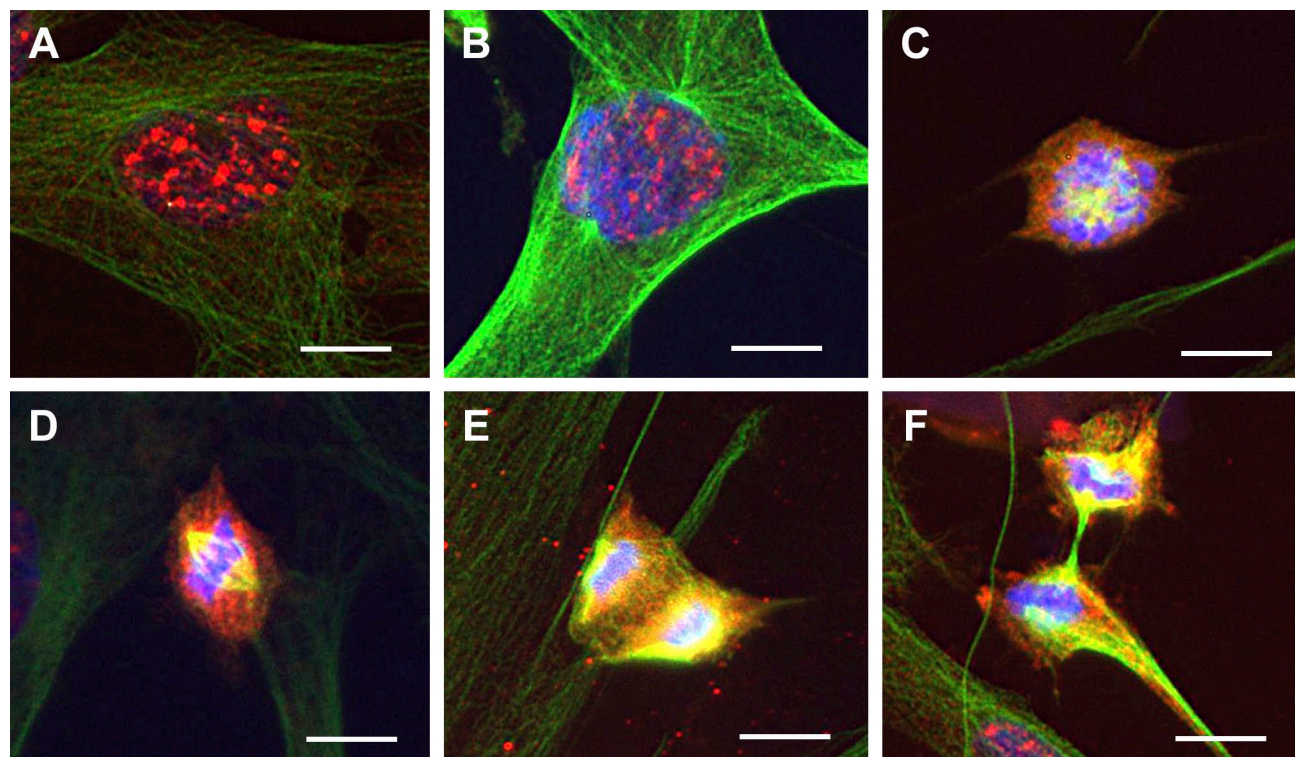


**Figure 4.** HAPLN1 redistributes from nucleus to cytosol during mitosis. HAPLN1 (red) and alpha tubulin (green). (A), interphase cells have strong nuclear staining. (B), in prophase, mitotic spindles begin forming and nuclear staining is diminished. In prometaphase through anaphase HAPLN1 is abundant in the cytosol (C, D) and in the midbody during telophase (E, F). Nuclei were stained with DAPI. Bar equals approximately 10  $\mu\text{m}$ . Abbreviations: DAPI, 4',6-diamidino-2-phenylindole; HAPLN1, hyaluronan and proteoglycan link protein 1.

within heavy plaque-like deposits of HAPLN1 left on the substrate (Fig. 8B). Fig. 8B also shows an example of a deposit of HAPLN1 that is similar in size and shape to the nearby nucleus. Punctuate deposits of HAPLN1 were usually seen underneath lamellipodia (Fig. 8C). Fig. 8D shows HAPLN1 colocalizing with connecting nodes under a mature actin network in a broad lamellipodium of a quiescent fibroblast, suggesting it may play a role in adhesion in these cells. Co-staining with tubulin revealed no particular colocalization or juxtapositional relationship of HAPLN1 with microtubules in the cytoplasm (see below).

#### *Addition of Exogenous HABP Induces Myofibroblast Formation*

We previously found that culturing dermal fibroblasts with recombinant versican G1 domain resulted in reorganization of the hyaluronan into cables.<sup>28</sup> Given the role of HAPLN1 in stabilizing the ECM and protecting hyaluronan from degradation, we wondered if it would affect pericellular matrix organization when added exogenously. We also wanted to know if cells would

take up exogenous HAPLN1 into their cytoplasm and nucleus.

A convenient source of exogenous HAPLN1 is the hyaluronan binding preparation HABP produced from bovine cartilage and used to localize hyaluronan. The preparation contains HAPLN1, together with the trypsin-resistant G1 domain fragment from aggrecan in approximately equal ratios. We used a non-biotinylated preparation to add to cells, and then the biotinylated preparation to look at subsequent effects on hyaluronan organization in the matrix. The monoclonal antibody to HAPLN1 was used to localize where the added HAPLN1 in the mixture was bound.

In HLFs incubated with HABP for 48 hr, cytoplasmic and nuclear staining for HAPLN1 was qualitatively similar to control cells and there did not appear to be any uptake of additional HAPLN1 by the cells, either into the cytoplasm or the nucleus, and no difference was seen cells in 0.1% FBS vs. 10% FBS (data not shown). In addition, the intracellular HAPLN1 showed no apparent relationship to microtubules (Fig. 9). Instead the added HAPLN1 was deposited on the substrate and gathered into clumps in the ECM and cell

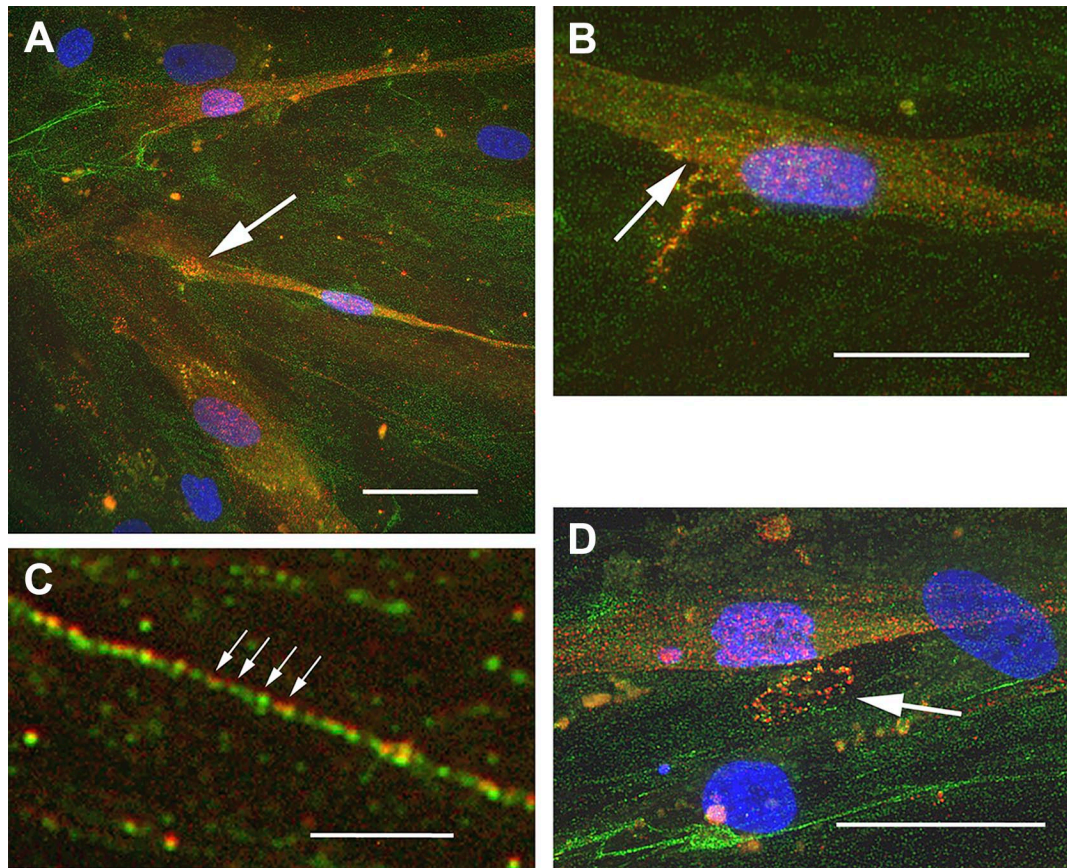


**Figure 5.** HAPLN1 colocalizes with versican along hyaluronan strands and in adhesive structures. HLFs growing in 10% FBS were stained for HAPLN1 (red) and versican (green). (A, B, and D) larger arrows indicate colocalization in deposits, some near and shaped like the nucleus. (C) Small arrows indicate the close juxtaposition of signals interspersed along a putative strand of hyaluronan. Nuclei were stained with DAPI. Bars equal 25  $\mu\text{m}$  in (A, B, and D), and 1  $\mu\text{m}$  in (C). Abbreviations: DAPI, 4',6-diamidino-2-phenylindole; FBS, fetal bovine serum; HAPLN1, hyaluronan and proteoglycan link protein 1; HLF, human lung fibroblasts.

surface (Fig. 9A). However, by phase contrast microscopy, pronounced stress fibers were observed in the cells that were incubated with HABP (Fig. 9B and D, arrowheads).

This prompted subsequent staining for  $\alpha$ -SMA (Fig. 10), which revealed that HABP treatment induced myofibroblast formation, whereas treatment with purified full-length versican had no effect. Quantitation of staining intensity, normalized as pixels per cell, indicated a dramatic and significant upregulation of  $\alpha$ -SMA in the cells treated with the HABP mixture of HAPLN1 and aggrecan G1 for 4 days. Similar results were seen in cells that had been plated for 4 days before addition of HABP (data not shown), although there tended to be higher  $\alpha$ -SMA staining in the control cells when they had been cultured for longer periods.

As mentioned, there were few, if any, ECM cables present in these cultures. Therefore, as a measure of the organization of the pericellular matrix, we quantified

ECM staining by measuring the pixel density of the hyaluronan-rich ECM within circumscribed regions of interest outside the cell as shown in Fig. 11. A lower pixel density indicates less hyaluronan or less compaction of the ECM. The ECM staining density was significantly greater in the HABP-treated cells. The addition of versican on the other hand, resulted in less hyaluronan staining in the pericellular matrix. This suggests there could be either increased amounts of the hyaluronan or a stiffening effect on the hyaluronan network in the ECM when globular hyaluronan binding proteins such as HAPLN1 and aggrecan G1 are added to growing fibroblasts.

## Discussion

We found that HAPLN1 is present on hyaluronan and alongside versican in the pericellular matrix, suggesting it plays a similar role in stabilizing the interaction of versican with hyaluronan of HLFs, as it does with



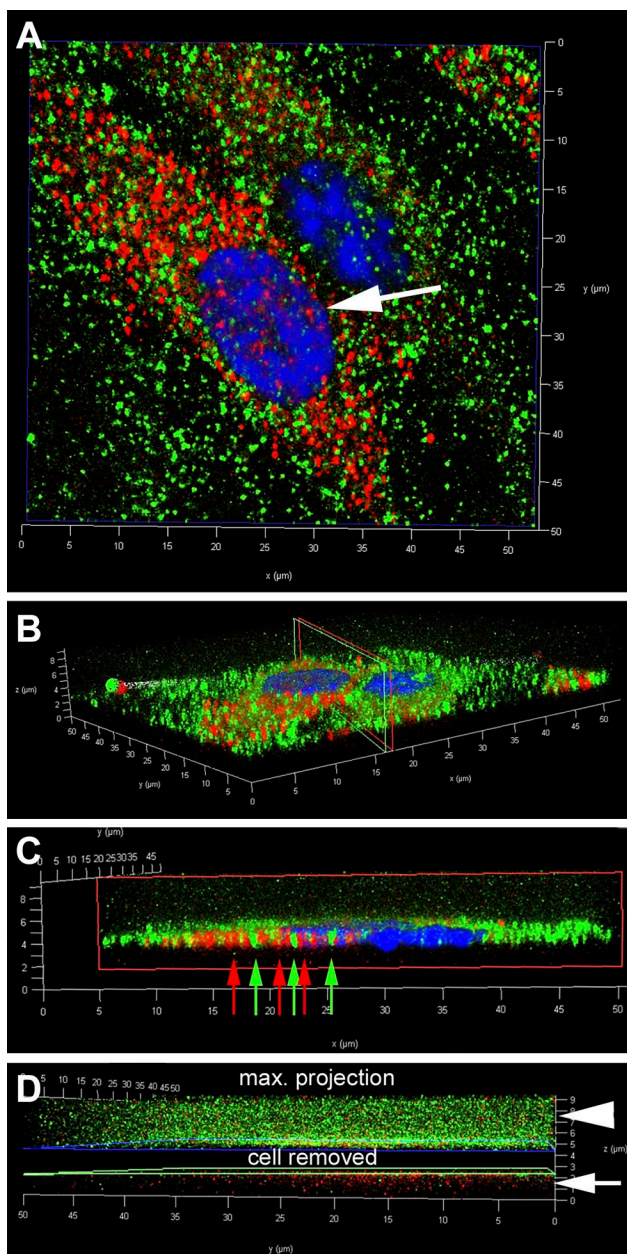


**Figure 6.** Versican and HAPLN1 distribution. Confocal microscopy and 3D image analysis of HLFs in 10% FBS stained for HAPLN1 (red) and versican (green). (A) *en face* view in an optical section midway through the plane of the nucleus, showing HAPLN1 and versican are present in the nucleus (arrow). (B) oblique view indicating the plane of the image stack for the horizontal slice shown in (C). Arrows indicate the closely juxtaposed cytoplasmic deposits that are positive for versican and HAPLN1. (D) a maximum side view projection of the entire field with the cell removed to show apical and basal pericellular matrix. Note how versican dominates in the matrix above the cells (arrow-head), while HAPLN1 has relatively more signal underneath the cells (arrow). Nuclei were stained with DAPI. Scale is indicated. Abbreviations: DAPI, 4',6-diamidino-2-phenylindole; FBS, fetal bovine serum; HAPLN1, hyaluronan and proteoglycan link protein I; HLF, human lung fibroblasts.

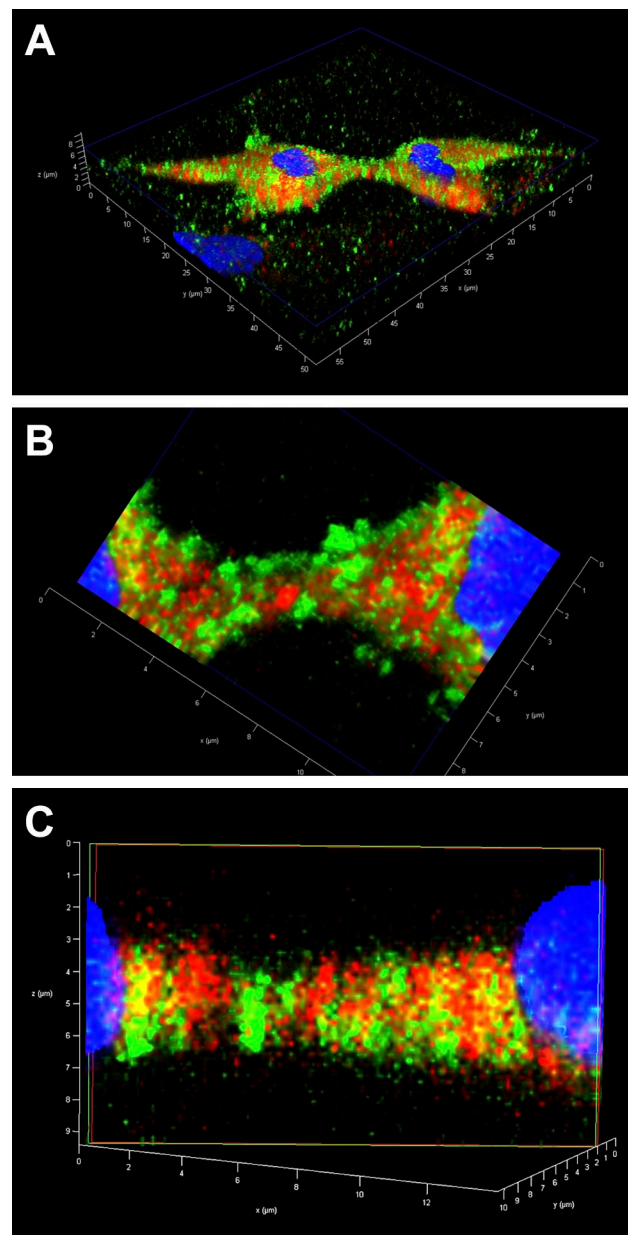


**Figure 7.** HAPLN1 (red) and versican (green) in mitotic cells. (A) oblique view of a confocal image stack of mitotic cells in telophase. (B) top view of the connecting midbody. (C) side view of the midbody. Nuclei were stained with DAPI. Scale is indicated. Abbreviations: DAPI, 4',6-diamidino-2-phenylindole; HAPLN1, hyaluronan and proteoglycan link protein I.

aggrecan in the chondrocyte pericellular matrix and in PNNs in the brain.<sup>1-5</sup>

HAPLN1 deposits were found above cells in the versican-rich ECM with alternating punctate signals along strands of hyaluronan. These deposits were similar in size and spacing as those we reported for exogenous versican G1.<sup>28</sup> HAPLN1 also colocalized with fragments of f-actin and with versican at

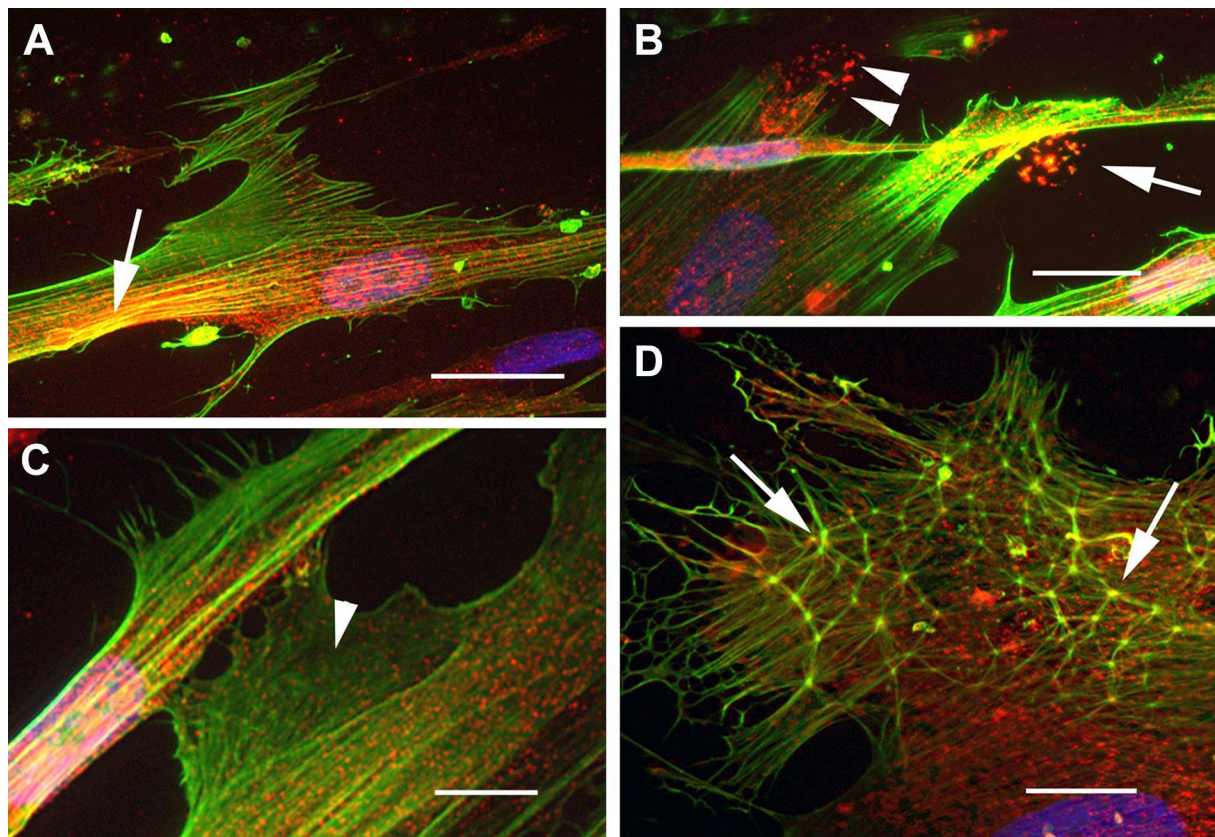


**Figure 8.** HLFs stained for HAPLN1 (red) and f-actin (green). (A to C), HLFs growing in 10% FBS. The arrows point to areas of partial colocalization. The arrowheads in (B) indicate an oval-shaped deposit of HAPLN1 that resembles the nucleus in the lower left of the image. The arrowhead in (C) points to a few HAPLN1 signals under a lamellipodium. (D) TGF- $\beta$ 1-induced myofibroblast. Note the co-localization of HAPLN1 under the connecting nodes of a mature actin network. Nuclei were stained with DAPI. Bars equal 25  $\mu$ m. Abbreviations: DAPI, 4',6-diamidino-2-phenylindole; FBS, fetal bovine serum; HAPLN1, hyaluronan and proteoglycan link protein 1; HLF, human lung fibroblasts; TGF- $\beta$ 1, tumor growth factor  $\beta$ 1.

plaque-like deposits which were frequently near and shaped like a nucleus and gave a distinct impression that the cell had moved, leaving behind a concentrated deposit. The staining did not resemble focal adhesions, however. We previously found that hyaluronidase digestion of the ECM caused retraction specifically of cortical actin between stress fibers and CD44 in the membrane,<sup>18</sup> and in the present study found HAPLN1 under actin networks rather than at the tips of stress fibers. The association of hyaluronan and CD44 with cortical actin,<sup>18</sup> the presence of hyaluronan and versican between stress fibers,<sup>29</sup> and the relative abundance of HAPLN1 under cell lamellipodia suggests HAPLN1 may play a role in stabilizing cell adhesion in some fashion.

All three members of the complex between hyaluronan,<sup>19</sup> versican,<sup>30</sup> and HAPLN1 (present study) have now been localized to the nucleus in fibroblasts, suggesting that the presence of HAPLN1 may be

important for nuclear structure or function. In addition, HAPLN1 was juxtaposed with versican in cytoplasmic vesicles inside the cell, indicating that link-stabilization may be important for any potential intracellular function of this complex. This is a novel finding, as there are very little data on HAPLN1 in fibroblasts. This is another example of these related ECM components being found in an intracellular location in fibroblasts, raising the possibility that there may be roles for these components both outside and inside cells.

Previous studies have shown that hyaluronan<sup>13,18,31</sup> and versican<sup>32</sup> can impact myofibroblast formation, but the effect of HAPLN1 has not been examined. A higher proportion of nuclei were positive for HAPLN1 staining in quiescent cells and TGF- $\beta$ -induced myofibroblasts compared to cells rapidly dividing in 10% FBS, and versican was closely associated with HAPLN1. HAPLN1 and versican were clearly present in deposits found within the plane of the nucleus,

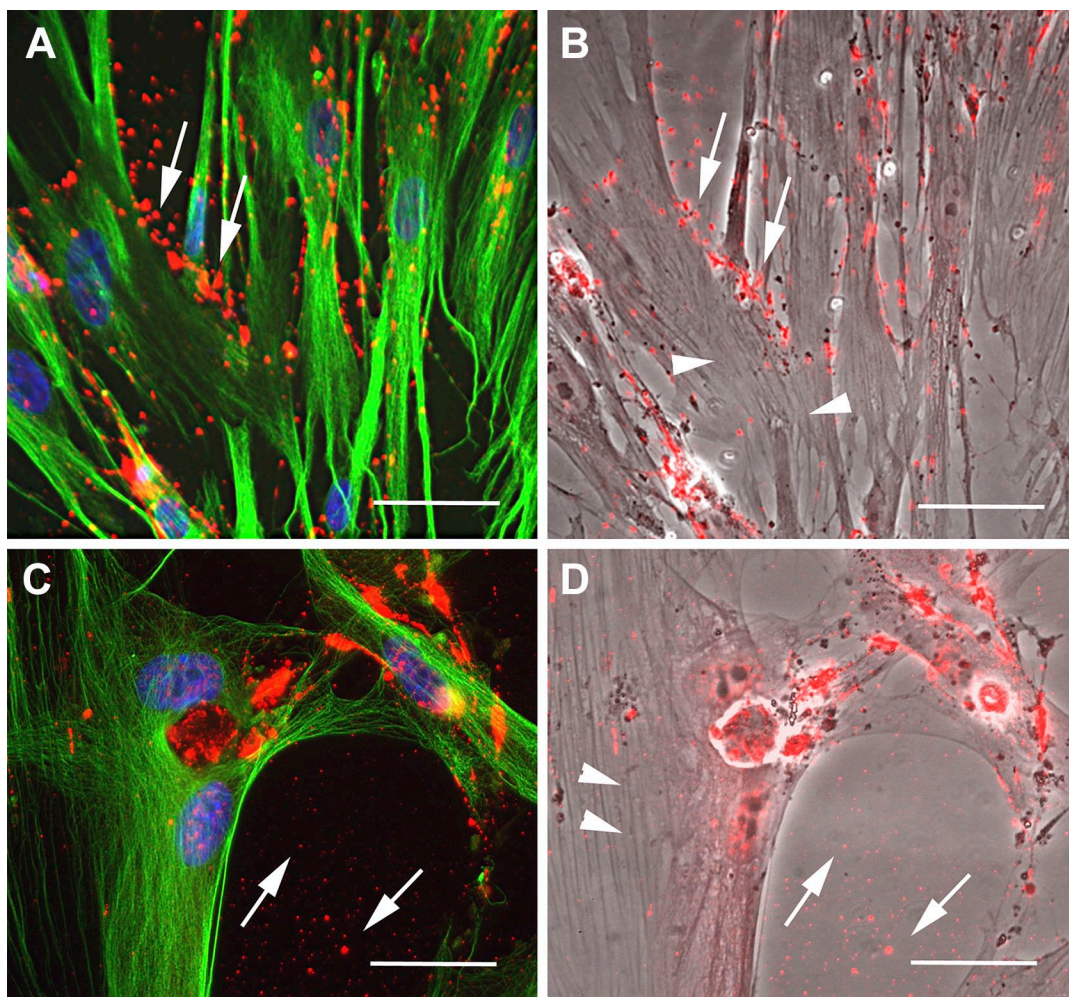


**Figure 9.** Exogenous HAPLN1 is reorganized and does not colocalize with tubulin. HABP was added to HLFs in the presence of 10% FBS and HAPLN1 (red) and alpha tubulin (green) detected by immunostaining after 4 days (A and C). No increased HAPLN1 signal was seen inside cells, suggesting not much is taken up by the cells. Instead, the HAPLN1 was gathered into clumps in the pericellular matrix (arrows). (B and D), phase contrast images of the same fields (merged with the link protein image). Note the large stress fibers inside the cells by phase contrast (arrowheads). Nuclei were stained with DAPI. Bars equal 25  $\mu$ m. Abbreviations: DAPI, 4',6-diamidino-2-phenylindole; FBS, fetal bovine serum; HABP, hyaluronan binding protein; HAPLN1, hyaluronan and proteoglycan link protein 1; HLF, human lung fibroblasts.

possibly invaginations or clefts, as was previously reported for intracellular hyaluronan<sup>19</sup> and versican.<sup>30</sup> In addition to PNNs,<sup>9</sup> HAPLN1 and hyaluronan were previously reported to be in the nucleus of neuronal cells.<sup>33</sup> However, the significance of nuclear and intracellular hyaladherins and an increase in nuclear HAPLN1 in myofibroblasts is not clear. Previous studies have suggested potential roles for intracellular hyaluronan, possibly through other intracellular binding partners.<sup>19,21,34–36</sup> Other studies have noted the presence of hyaluronan at the cleavage furrow in mitotic cells and the mitotic spindle (decorated with hyaluronan and its receptor, receptor for hyaluronic

acid-mediated motility (RHAMM)).<sup>19,21,37</sup> Large amounts of cell membrane (and probably ECM molecule bound to it) are rapidly retracted during mitotic cell rounding. The redistribution of HAPLN1 from nucleus to cytosol and strong cytoplasmic staining during mitosis may reflect, in part, the drawing in of membrane and any associated ECM as part of the cell rounding and chromatin condensation process. Another study found that disruption of versican expression interfered with mitosis in embryonic dermal fibroblasts.<sup>30</sup> However, more work will need to be done to determine if HAPLN1 disruption affects myofibroblast formation or cell proliferation.

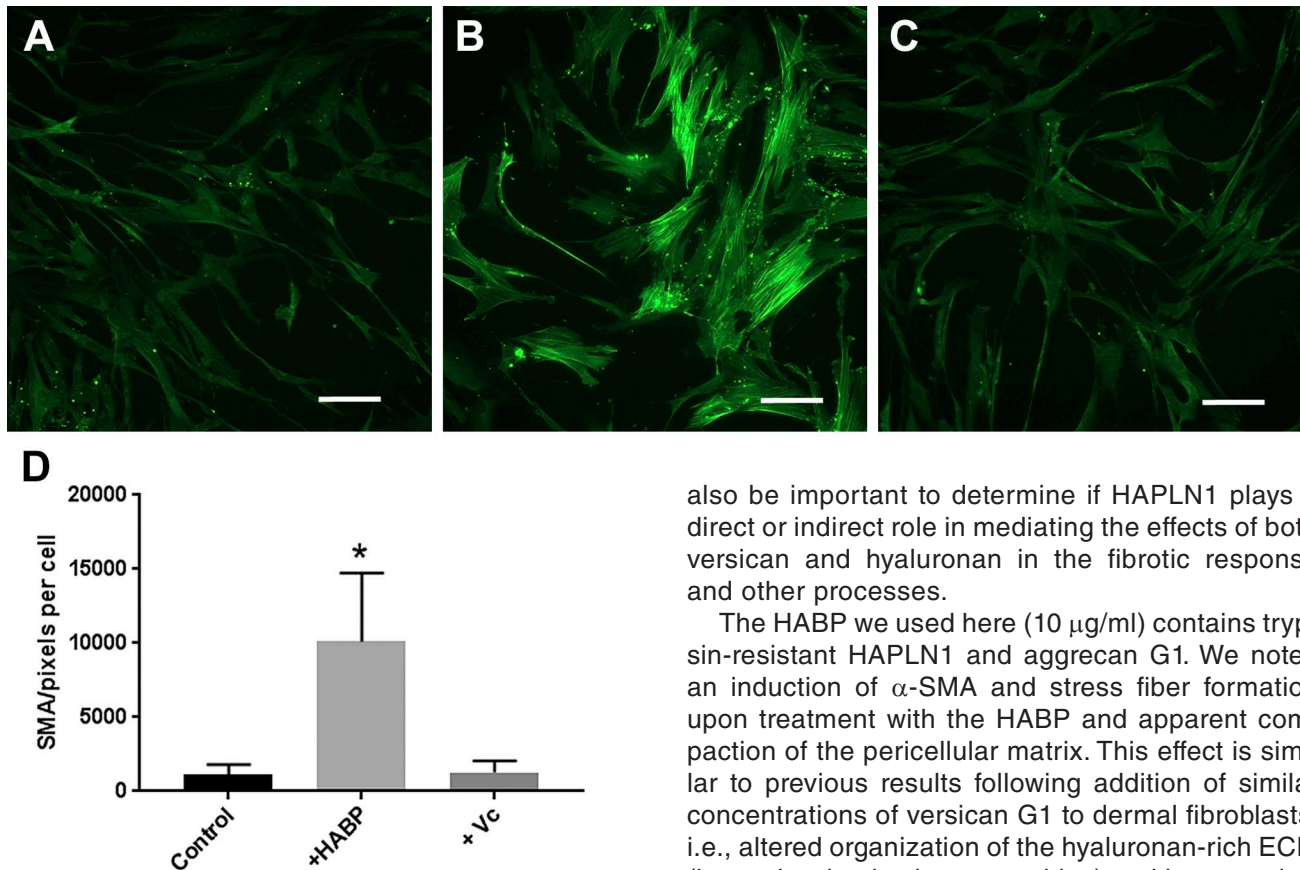


**Figure 10.** Alpha-SMA is increased by HABP treatment. (A), HLFs in 10% FBS alone; (B), cells treated with bovine HABP (HAPLN1 and G1), and (C), full length bovine versican were immunostained for  $\alpha$ -SMA (green). (D), shows quantitation of  $\alpha$ -SMA staining intensity per cell.  $N=10$  fields per condition. Bars equal 50  $\mu$ m. Abbreviations: HABP, hyaluronan binding protein; HAPLN1, hyaluronan and proteoglycan link protein 1; HLF, human lung fibroblasts;  $\alpha$ -SMA,  $\alpha$ -smooth muscle actin.

Both hyaluronan and versican are important contributors to the development of lung diseases, including fibrosis.<sup>12-14,38,39</sup> The role of hyaluronan and its binding partners in myofibroblast conversion and lung fibrosis is complex because they are part of the fibrotic ECM, and also directly impact the activation and trafficking of leukocytes during the inflammatory response.<sup>40-45</sup> It should be noted that our experiments were conducted in medium containing high (25 mM) glucose, which tends to promote formation of leukocyte adhesive hyaluronan matrices and intracellular hyaluronan during inflammatory processes.<sup>46</sup> This could potentially result in abnormally high intracellular levels of HAPLN1. We do yet not know if the intracellular and nuclear HAPLN1 distribution reported here or synthesis will change with altered glucose concentrations. It will

also be important to determine if HAPLN1 plays a direct or indirect role in mediating the effects of both versican and hyaluronan in the fibrotic response and other processes.

The HABP we used here (10  $\mu$ g/ml) contains trypsin-resistant HAPLN1 and aggrecan G1. We noted an induction of  $\alpha$ -SMA and stress fiber formation upon treatment with the HABP and apparent compaction of the pericellular matrix. This effect is similar to previous results following addition of similar concentrations of versican G1 to dermal fibroblasts, i.e., altered organization of the hyaluronan-rich ECM (by coalescing hyaluronan cables) and increased  $\alpha$ -SMA protein expression.<sup>28</sup> However, actual local cellular level concentrations of HAPLN1 at different regions on the cell membrane or perinuclear inclusions are difficult to estimate. We cannot rule out that this just represents more hyaluronan in the pericellular matrix. Another study used a similar HABP preparation (which they termed metastatin) to stop cancer cells from growing.<sup>47</sup> Given their high homology, adding any one of these globular domains should result in similar physical effects on hyaluronan. For example, it was shown previously by electron microscopy that addition of either HAPLN1 or aggrecan G1 caused shortening and, potentially stiffening of hyaluronan chains,<sup>48</sup> or disruption of the hyaluronan network.<sup>49</sup>

ECM stiffness is a known regulator of myofibroblast formation.<sup>50</sup> Chen and Thibeault showed that 2D and 3D hyaluronan-rich ECMs inhibited  $\alpha$ -SMA production in response to TGF- $\beta$ 1 due to reduced stiffness.<sup>51</sup> A distinction should be made between overall ECM stiffness, in which collagen fibers tend to dominate and stiffness of the hyaluronan network itself. Hyaladherins, such as HAPLN1 and others, may play roles in modifying material properties of hyaluronan-rich ECMs. In the present study, addition of HAPLN1 and G1 caused apparent ECM

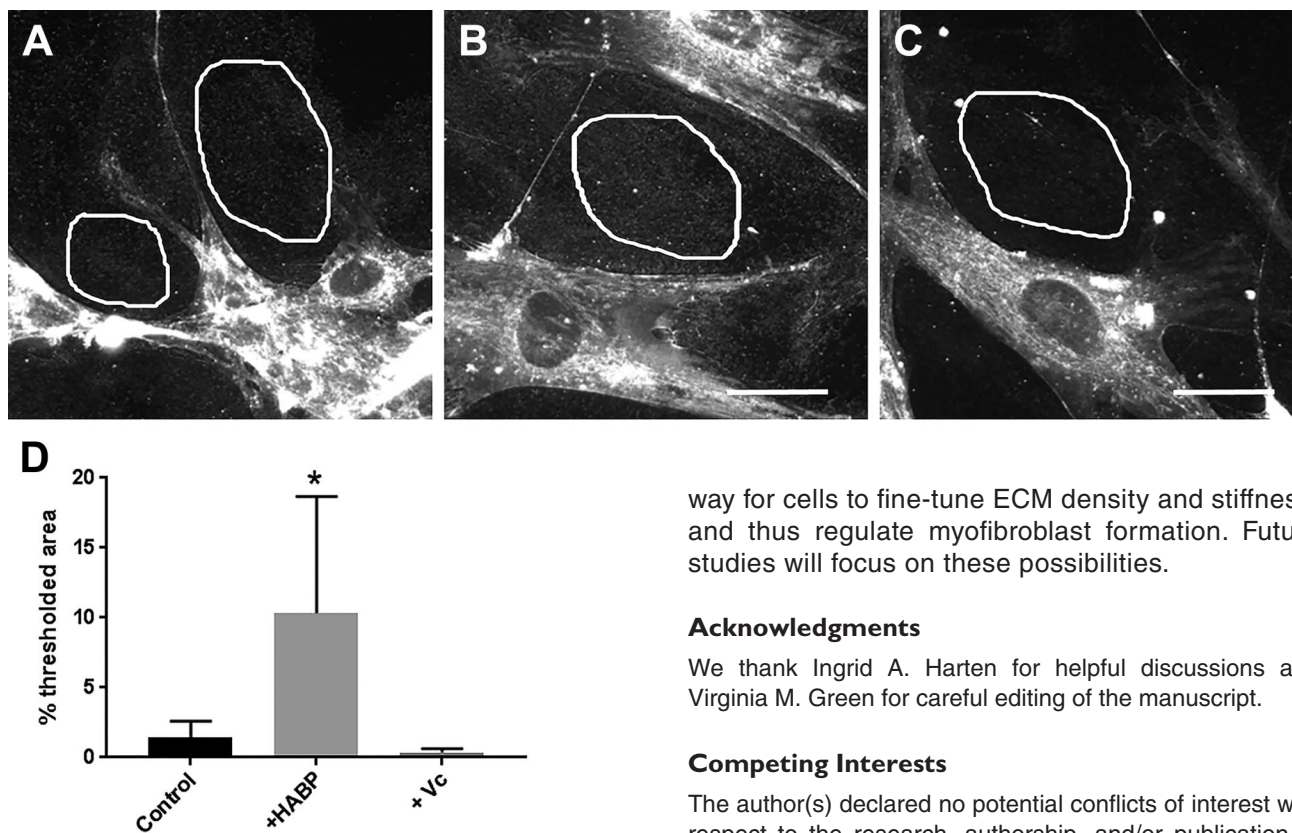


**Figure 11.** Pericellular matrix compaction is increased by HAPLN1. Hyaluronan staining in (A) control; (B) HAPB-treated; and (C) versican-treated cells. The outlines indicate examples of regions of interest selected for quantitation of staining density of the pericellular matrix. (D) percent of the area stained for hyaluronan in each treatment as a measure of matrix compaction. Bar equals 25  $\mu$ m. Abbreviations: HAPB, hyaluronan binding protein; HAPLN1, hyaluronan and proteoglycan link protein I.

compaction and increased  $\alpha$ -SMA staining, while full-length versican did not have the compaction effect and did not promote myofibroblast formation in HLFs. Another study reported that an overabundance of cell-derived versican in the ECM, due to lack of metalloprotease cleavage, promoted myofibroblast formation in mouse dermal fibroblasts.<sup>52</sup> The hyaladherin TNF $\alpha$ -stimulated gene-6 (TSG-6) was shown to crosslink hyaluronan and rigidify hyaluronan films.<sup>53</sup> Interestingly, CD44, the receptor for hyaluronan, is more fluid in the membrane of fibroblasts versus myofibroblasts<sup>54</sup> raising the question of whether increased cell-associated HAPLN1 following TGF- $\beta$ 1 induction stabilizes the ECM and could affect CD44 fluidity and cortical actin from outside the cell. Our results suggest that altering ratios of full-length versican to HAPLN1 (or other proteoglycan fragments that bind to hyaluronan) may be a

way for cells to fine-tune ECM density and stiffness, and thus regulate myofibroblast formation. Future studies will focus on these possibilities.

#### Acknowledgments

We thank Ingrid A. Harten for helpful discussions and Virginia M. Green for careful editing of the manuscript.

#### Competing Interests

The author(s) declared no potential conflicts of interest with respect to the research, authorship, and/or publication of this article.

#### Author Contributions

SPE conceived and performed experiments, microscopy, data analysis, and drafted the manuscript; IK assisted with tissue culture and analyses; CKC purified and analyzed HAPB; MDG performed confocal microscopy; RBV administers the imaging core, TNW edited the manuscript and obtained funding. All authors have contributed to the final version of the manuscript. All authors approved the final manuscript.

#### Funding

The author(s) disclosed receipt of the following financial support for the research, authorship, and/or publication of this article: This study was supported by a grant from the Heidner Foundation and National Institutes of Health grants R01 HL128361, R01 AI 130280, and U19 AI125378 to T.N.W.

#### Data Accessibility Statement

All relevant data are included in the manuscript. Any underlying data not shown can be accessed by contacting the authors directly.

#### Literature Cited

- Hardingham TE, Muir H. The specific interaction of hyaluronic acid with cartilage proteoglycans. *Biochim Biophys Acta.* 1972;279:401–5.

2. Oegema TR Jr, Laidlaw J, Hascall VC, Dziewiatkowski DD. The effect of proteoglycans on the formation of fibrils from collagen solutions. *Arch Biochem Biophys.* 1975;170:698–709.
3. Rauch U, Hirakawa S, Oohashi T, Kappler J, Roos G. Cartilage link protein interacts with neurocan, which shows hyaluronan binding characteristics different from CD44 and TSG-6. *Matrix Biol.* 2004;22:629–39.
4. Shi S, Grothe S, Zhang Y, O'Connor-McCourt MD, Poole AR, Roughley PJ, Mort JS. Link protein has greater affinity for versican than aggrecan. *J Biol Chem.* 2004;279:12060–6.
5. Kwok JC, Carulli D, Fawcett JW. In vitro modeling of perineuronal nets: hyaluronan synthase and link protein are necessary for their formation and integrity. *J Neurochem.* 2010;114:1447–59.
6. Lyon M, Nieduszynski IA. A study of equilibrium binding of link protein to hyaluronate. *Biochem J.* 1983;213:445–50.
7. Rosenberg L, Tang LH, Pal S, Johnson TL, Choi HU. Proteoglycans of bovine articular cartilage. Studies of the direct interaction of link protein with hyaluronate in the absence of proteoglycan monomer. *J Biol Chem.* 1988;263:18071–7.
8. Czipri M, Otto JM, Cs-Szabo G, Kamath RV, Vermes C, Firneisz G, Kolman KJ, Watanabe H, Li Y, Roughley PJ, Yamada Y, Olsen BR, Glant TT. Genetic rescue of chondrodysplasia and the perinatal lethal effect of cartilage link protein deficiency. *J Biol Chem.* 2003;278:39214–23.
9. Carulli D, Pizzorusso T, Kwok JC, Putignano E, Poli A, Forostyak S, Andrews MR, Deepa SS, Glant TT, Fawcett JW. Animals lacking link protein have attenuated perineuronal nets and persistent plasticity. *Brain.* 2010;133:2331–47.
10. Kaur A, Ecker BL, Douglass SM, Kugel CH 3rd, Webster MR, Almeida FV, Somasundaram R, Hayden J, Ban E, Ahmadzadeh H, Franco-Barraza J, Shah N, Mellis IA, Keeney F, Kossenkov A, Tang HY, Yin X, Liu Q, Xu X, Fane M, Brafford P, Herlyn M, Speicher DW, Wargo JA, Tetzlaff MT, Haydu LE, Raj A, Shenoy V, Cukierman E, Weeraratna AT. Remodeling of the collagen matrix in aging skin promotes melanoma metastasis and affects immune cell motility. *Cancer Discov.* 2019;9:64–81.
11. Ecker BL, Kaur A, Douglass SM, Webster MR, Almeida FV, Marino GE, Sinnamon AJ, Neuwirth MG, Alicea GM, Ndoye A, Fane M, Xu X, Sim MS, Deutsch GB, Faries MB, Karakousis GC, Weeraratna AT. Age-related changes in HAPLN1 increase lymphatic permeability and affect routes of melanoma metastasis. *Cancer Discov.* 2019;9:82–95.
12. Jenkins RH, Thomas GJ, Williams JD, Steadman R. Myofibroblastic differentiation leads to hyaluronan accumulation through reduced hyaluronan turnover. *J Biol Chem.* 2004;279:41453–60.
13. Webber J, Jenkins RH, Meran S, Phillips A, Steadman R. Modulation of TGF $\beta$ 1-dependent myofibroblast differentiation by hyaluronan. *Am J Pathol.* 2009;175:148–60.
14. Webber J, Meran S, Steadman R, Phillips A. Hyaluronan orchestrates transforming growth factor- $\beta$ 1-dependent maintenance of myofibroblast phenotype. *J Biol Chem.* 2009;284:9083–92.
15. Spanjer AI, Baarsma HA, Oostenbrink LM, Jansen SR, Kuipers CC, Lindner M, Postma DS, Meurs H, Heijink IH, Gosens R, Konigshoff M. TGF- $\beta$ -induced profibrotic signaling is regulated in part by the WNT receptor Frizzled-8. *FASEB J.* 2016;30:1823–35.
16. Estany S, Vicens-Zygmunt V, Llatjos R, Montes A, Penin R, Escobar I, Xaubet A, Santos S, Manresa F, Dorca J, Molina-Molina M. Lung fibrotic tenascin-C upregulation is associated with other extracellular matrix proteins and induced by TGF $\beta$ 1. *BMC Pulm Med.* 2014;14:120.
17. Venkatesan N, Roughley PJ, Ludwig MS. Proteoglycan expression in bleomycin lung fibroblasts: role of transforming growth factor- $\beta$ 1 and interferon- $\gamma$ . *Am J Physiol Lung Cell Mol Physiol.* 2002;283:L806–14.
18. Evanko SP, Potter-Perigo S, Petty LJ, Workman GA, Wight TN. Hyaluronan controls the deposition of fibronectin and collagen and modulates TGF- $\beta$ 1 induction of lung myofibroblasts. *Matrix Biol.* 2015;42:74–92.
19. Evanko SP, Angello JC, Wight TN. Formation of hyaluronan- and versican-rich pericellular matrix is required for proliferation and migration of vascular smooth muscle cells. *Arterioscler Thromb Vasc Biol.* 1999;19:1004–13.
20. Evanko SP, Wight TN. Intracellular localization of hyaluronan in proliferating cells. *J Histochem Cytochem.* 1999;47:1331–42.
21. Evanko SP, Parks WT, Wight TN. Intracellular hyaluronan in arterial smooth muscle cells: association with microtubules, RHAMM, and the mitotic spindle. *J Histochem Cytochem.* 2004;52:1525–35.
22. Evanko SP, Johnson PY, Braun KR, Underhill CB, Dudhia J, Wight TN. Platelet-derived growth factor stimulates the formation of versican-hyaluronan aggregates and pericellular matrix expansion in arterial smooth muscle cells. *Arch Biochem Biophys.* 2001;394:29–38.
23. LeBaron RG, Zimmermann DR, Ruoslahti E. Hyaluronate binding properties of versican. *J Biol Chem.* 1992;267:10003–10.
24. Underhill CB, Nguyen HA, Shizari M, Culty M. CD44 positive macrophages take up hyaluronan during lung development. *Dev Biol.* 1993;155:324–36.
25. Olin AI, Morgelin M, Sasaki T, Timpl R, Heinegard D, Asperger A. The proteoglycans aggrecan and Versican form networks with fibulin-2 through their lectin domain binding. *J Biol Chem.* 2001;276:1253–61.
26. Evanko SP, Chan CK, Johnson PY, Frevert CW, Wight TN. The biochemistry and immunohistochemistry of versican. In: Mecham RP, editor. *Methods in extracellular matrix biology. Methods in cell biology.* 143. Cambridge, MA: Academic Press; 2018. p. 261–79.
27. Raghu G, Chen YY, Rusch V, Rabinovitch PS. Differential proliferation of fibroblasts cultured from normal and fibrotic human lungs. *Am Rev Respir Dis.* 1988;138:703–8.
28. Merrilees MJ, Zuo N, Evanko SP, Day AJ, Wight TN. G1 domain of versican regulates hyaluronan organization

- and the phenotype of cultured human dermal fibroblasts. *J Histochem Cytochem*. 2016;64:353–63.
29. Yamagata M, Saga S, Kato M, Bernfield M, Kimata K. Selective distributions of proteoglycans and their ligands in pericellular matrix of cultured fibroblasts. Implications for their roles in cell-substratum adhesion. *J Cell Sci*. 1993;106:55–65.
  30. Carthy JM, Abraham T, Meredith AJ, Boroomand S, McManus BM. Versican localizes to the nucleus in proliferating mesenchymal cells. *Cardiovasc Pathol*. 2015; 24:368–74.
  31. Meran S, Thomas DW, Stephens P, Enoch S, Martin J, Steadman R, Phillips AO. Hyaluronan facilitates transforming growth factor-beta1-mediated fibroblast proliferation. *J Biol Chem*. 2008;283:6530–45.
  32. Carthy JM, Meredith AJ, Boroomand S, Abraham T, Luo Z, Knight D, McManus BM. Versican V1 overexpression induces a myofibroblast-like phenotype in cultured fibroblasts. *PLoS ONE*. 2015;10:e0133056.
  33. Ripellino JA, Margolis RU, Margolis RK. Immunoelectron microscopic localization of hyaluronic acid-binding region and link protein epitopes in brain. *J Cell Biol*. 1989;108:1899–907.
  34. Grammatikakis N, Grammatikakis A, Yoneda M, Yu Q, Banerjee SD, Toole BP. A novel glycosaminoglycan-binding protein is the vertebrate homologue of the cell cycle control protein, Cdc37. *J Biol Chem*. 1995;270: 16198–205.
  35. Deb TB, Datta K. Molecular cloning of human fibroblast hyaluronic acid-binding protein confirms its identity with P-32, a protein co-purified with splicing factor SF2. Hyaluronic acid-binding protein as P-32 protein, co-purified with splicing factor SF2. *J Biol Chem*. 1996; 271:2206–12.
  36. Hascall VC, Majors AK, De La Motte CA, Evanko SP, Wang A, Drazba JA, Strong SA, Wight TN. Intracellular hyaluronan: a new frontier for inflammation? *Biochim Biophys Acta*. 2004;1673:3–12.
  37. Tammi R, Tammi M. Correlations between hyaluronan and epidermal proliferation as studied by [<sup>3</sup>H]glucosamine and [<sup>3</sup>H]thymidine incorporations and staining of hyaluronan on mitotic keratinocytes. *Exp Cell Res*. 1991;195:524–7.
  38. Wight TN, Kang I, Evanko SP, Harten IA, Chang MY, Pearce OMT, Allen CE, Frevert CW. Versican—a critical extracellular matrix regulator of immunity and inflammation. *Front Immunol*. 2020;11:512.
  39. Merrilees MJ, Ching PST, Beaumont B, Hinek A, Wight TN, Black PN. Changes in elastin, elastin binding protein and versican in alveoli in chronic obstructive pulmonary disease. *Respir Res*. 2008;9:41.
  40. Mummert ME, Mohamadzadeh M, Mummert DI, Mizumoto N, Takashima A. Development of a peptide inhibitor of hyaluronan-mediated leukocyte trafficking. *J Exp Med*. 2000;192:769–79.
  41. Potter-Perigo S, Johnson PY, Evanko SP, Chan CK, Braun KR, Wilkinson TS, Altman LC, Wight TN. Polyinosine-polycytidylic acid stimulates versican accumulation in the extracellular matrix promoting monocyte adhesion. *Am J Respir Cell Mol Biol*. 2010;43:109–20.
  42. Bollyky PL, Falk BA, Wu RP, Buckner JH, Wight TN, Nepom GT. Intact extracellular matrix and the maintenance of immune tolerance: high molecular weight hyaluronan promotes persistence of induced CD4+CD25+ regulatory T cells. *J Leukoc Biol*. 2009;86:567–72.
  43. Bollyky PL, Evanko SP, Wu RP, Potter-Perigo S, Long SA, Kinsella BD, Reijonen H, Guebtner K, Teng B, Chan CK, Braun KR, Gebe JA, Nepom GT, Wight TN. Th1 cytokines promote T-cell binding to antigen-presenting cells via enhanced hyaluronan production and accumulation at the immune synapse. *Cell Mol Immunol*. 2010;7:211–20.
  44. Evanko SP, Potter-Perigo S, Bollyky PL, Nepom GT, Wight TN. Hyaluronan and versican in the control of human T-lymphocyte adhesion and migration. *Matrix Biol*. 2012;31:90–100.
  45. Gaucherand L, Falk BA, Evanko SP, Workman G, Chan CK, Wight TN. Crosstalk between T lymphocytes and lung fibroblasts: generation of a hyaluronan-enriched extracellular matrix adhesive for monocytes. *J Cell Biochem*. 2017;118:2118–30.
  46. Wang A, de la Motte C, Lauer M, Hascall V. Hyaluronan matrices in pathobiological processes. *FEBS J*. 2011; 278:1412–8.
  47. Liu N, Lapcevic RK, Underhill CB, Han Z, Gao F, Swartz G, Plum SM, Zhang L, Green SJ. Metastatin: a hyaluronan-binding complex from cartilage that inhibits tumor growth. *Cancer Res*. 2001;61:1022–8.
  48. Morgelin M, Paulsson M, Heinegard D, Aebi U, Engel J. Evidence of a defined spatial arrangement of hyaluronate in the central filament of cartilage proteoglycan aggregates. *Biochem J*. 1995;307(Pt 2):595–601.
  49. Brewton RG, Mayne R. Mammalian vitreous humor contains networks of hyaluronan molecules: electron microscopic analysis using the hyaluronan-binding region (G1) of aggrecan and link protein. *Exp Cell Res*. 1992;198:237–49.
  50. Hinz B, Gabbiani G. Fibrosis: recent advances in myofibroblast biology and new therapeutic perspectives. *F1000 Biol Rep*. 2010;2:78.
  51. Chen X, Thibeault SL. Response of fibroblasts to transforming growth factor-β1 on two-dimensional and in three-dimensional hyaluronan hydrogels. *Tissue Eng Part A*. 2012;18:2528–38.
  52. Islam S, Chuensirikulchai K, Khummuang S, Keratibumrunpong T, Kongtawelert P, Kasinrerak W, Hatano S, Nagamachi A, Honda H, Watanabe H. Accumulation of versican facilitates wound healing: implication of its initial ADAMTS-cleavage site. *Matrix Biol*. 2020;87:77–93.
  53. Baranova NS, Nileback E, Haller FM, Briggs DC, Svedhem S, Day AJ, Richter RP. The inflammation-associated protein TSG-6 cross-links hyaluronan via hyaluronan-induced TSG-6 oligomers. *J Biol Chem*. 2011;286:25675–86.
  54. Midgley AC, Rogers M, Hallett MB, Clayton A, Bowen T, Phillips AO, Steadman R. Transforming growth factor-β1 (TGF-β1)-stimulated fibroblast to myofibroblast differentiation is mediated by hyaluronan (HA)-facilitated epidermal growth factor receptor (EGFR) and CD44 co-localization in lipid rafts. *J Biol Chem*. 2013;288:14824–38.